Journal of Heat and Mass Transfer Research 13 (2026), Serial Number 26, 175 – 192

Semnan University

Journal of Heat and Mass Transfer Research

Journal homepage: https://jhmtr.semnan.ac.ir

ISSN: 2383-3068

Research Article

Experimental Optimization of Hybrid Nanoparticle-Enhanced Biodiesel–Diesel Blends for Engine Performance and Fuel Stability

Seyed Amir Hossein Zamzamian *, **Marjan Mehrali**

Energy Department, Materials and Energy Research Center(MERC), Karaj, Iran

ARTICLE INFO

Article history:

Received: 2025-05-24

Revised: 2025-07-05

Accepted: 2025-07-24

Keywords:

Hybrid nano fuel;

Nanomaterial;

Nano biodiesel;

Physicochemical;

Properties;

Diesel engine.

ABSTRACT

This study investigates the effects of hybrid nanoparticles on the properties and performance of nano-biodiesel-diesel blends. Four types of nanoparticles (Al_2O_3, SiO_2, CuO, and Co_3O_4) were studied to determine the most stable hybrid nanofuel compositions. The biodiesel was produced from waste cooking oil using a transesterification method with methanol at a 9:1 molar ratio and potassium hydroxide as a catalyst. Five fuel blends were prepared and tested: pure diesel (D_{100}), pure biodiesel (B_{100}), B_{20} (20% biodiesel + 80% diesel), and two hybrid nanofuel blends ($B_{20}AS_{40}$ and $B_{20}ASCC_{40}$) containing different combinations of nanoparticles. Comprehensive physicochemical property analyses and engine performance tests were conducted. The results demonstrate significant improvements in fuel properties and engine performance. The calorific value increased by 7% for $B_{20}AS_{40}$ and 9% for $B_{20}ASCC_{40}$, compared to pure diesel. Brake specific fuel consumption decreased by 15% and 14%, respectively, for these nanofuel blends, while brake thermal efficiency improved to 31.1% and 32.0%, compared to 30.0% for pure diesel. These findings confirm that hybrid nanoparticles can effectively enhance fuel properties and engine performance when properly combined with biodiesel-diesel blends. The research provides valuable insights into developing more efficient and environmentally friendly fuel alternatives for diesel engines. Emission parameters such as NO_x, CO, and HC were not within the scope of this experimental setup and were therefore not measured.

1. Introduction

Diesel internal combustion engines are widely recognized for their high efficiency, making them a preferred choice for powering heavy-duty vehicles such as buses and trucks. The use of diesel engines in light vehicles has also been well received by consumers (Soudagar et al. 2024). According to the European Environmental Organization, the demand for heavy diesel fuel is projected to increase significantly in the coming years, while the demand for gasoline is expected to decline. Over the next decade, gasoline consumption is anticipated to decrease from 20% to 13%, whereas the demand for heavy diesel fuel is expected to reach 60% (Poliscanova 2017). Forecasts indicate that, between 2008 and 2028, the consumption of diesel fuel will double compared to gasoline-powered combustion engines. This transition has necessitated the development of facilities for light and heavy fuel separation in Europe, leading to an imbalance in fuel supply and demand and raising energy security concerns within the European Union

* **Corresponding author.**

E-mail address: azamzamian@merc.ac.ir

Cite this article as:

Zamzamian, S.A.H. and Mehrali, M., 2026. Experimental Optimization of Hybrid Nanoparticle-Enhanced Biodiesel–Diesel Blends for Engine Performance and Fuel Stability. *Journal of Heat and Mass Transfer Research*, 13(2), pp. 175-192.

https://doi.org/10.22075/JHMTR.2025.37866.1758

(Goh et al. 2020). Biofuels, particularly biodiesel, have emerged as a viable alternative to heavy diesel fuel due to their similar chemical and physical properties. International fuel standards such as EN590 regulate biodiesel specifications to ensure compatibility with conventional diesel engines (Bastawissi et al. 2019). One of the key challenges in biodiesel usage is maintaining fuel stability to enable efficient combustion at lower temperatures. Water content in biodiesel remains a well-documented issue affecting fuel performance (Rajak and Verma 2020). As a renewable and environmentally friendly fuel, biodiesel is increasingly viewed as the fuel of the future. Research efforts have focused on optimizing biodiesel production processes to enhance its viability as a sustainable alternative (Abed et al. 2018; El-Shenawy et al. 2019; Yesilyurt 2019). Among various production methods, catalytic transesterification has been identified as the most cost-effective approach. This method employs homogeneous catalysts to facilitate the conversion of waste cooking oil (WCO) into biodiesel, offering a commercially scalable solution with high efficiency (Milano et al. 2018). Prior studies have demonstrated that transesterification using homogeneous catalysts results in improved oxygen reaction kinetics and reduced combustion time (Elkelawy et al. 2021). Milano et al. (2018) investigated biodiesel production from a mixture of waste cooking oil and non-edible oil (WC70CI30). Their study revealed that degumming the feed-stock mixture enhances fuel quality by removing impurities. They also found that a combustion temperature above 65°C leads to methanol evaporation, thereby reducing the effectiveness of methanol as a catalyst. Using Design-Expert software, they determined that the optimal reaction time for biodiesel synthesis is 70 minutes. Additionally, the composition of saturated and unsaturated acids in the biofuel influences its cetane number, directly impacting ignition timing and greenhouse gas emissions. Notably, biodiesel exhibited higher viscosity compared to conventional diesel fuel (Abdollahi et al. 2020). The incorporation of nanoparticles in base fuels has been identified as a promising strategy to enhance fuel energy density and combustion efficiency. Nanoparticles function as catalysts, leveraging their high surface-to-volume ratio to improve fuel properties and optimize combustion (Chakraborty et al. 2019). Research on nanofluids has primarily focused on three main categories: metal-based (e.g., Cu, Fe, Au), metal oxide-based (e.g., TiO_2, Al_2O_3, CuO), and non-metallic carbon-based nanofluids (Madhesh and Kalaiselvam 2014). The addition of nanoparticles to conventional fuels (e.g., diesel, biodiesel, water, oil, and ethylene glycol) significantly alters their thermophysical properties, making them more efficient for combustion applications (Rostamian et al. 2017; Jana et al. 2007; Afrand 2017). Recent studies have explored the potential benefits of hybrid nanofluids, which combine multiple types of nanoparticles to achieve enhanced performance. The inclusion of solid nanoparticles in fuel fluids has been shown to increase heat transfer efficiency, although results vary depending on nanoparticle composition (Asadi M. and Asadi A. 2016; Esfe et al. 2016; Balla et al. 2013; Eshgarf & Afrand 2016). Hybrid nanoparticles have been developed to further optimize fuel characteristics, reducing costs while improving convective heat transfer efficiency (Esfe et al. 2018; Hemmat Esfe et al. 2017). However, some studies have reported minimal or no improvement in fuel properties when using hybrid nanoparticles (Jana et al. 2007). The industrial application of nanoparticles remains an area of active research, with stability, heat transfer, and chemical properties being critical factors for commercialization. Stability is particularly crucial as nanoparticle sedimentation in fuel systems can lead to efficiency losses. Ensuring long-term suspension stability is a key challenge in nanofuel applications, prompting researchers to investigate various stabilization techniques (Balamurugan and Sajith 2017; Mahajan 2017; Mehta et al. 2015; Hazrat et al. 2019). Saxena et al. (2019) examined the performance of a biodiesel-diesel blend (60% diesel, 40% biodiesel) with varying concentrations of TiO_2 nanoparticles in a 3.5 kW diesel engine. Their study demonstrated that the optimal nanoparticle concentration (150 mg/L) significantly enhanced engine performance, with improvements of 3.25% in brake thermal efficiency (BTE) and a 42.18% reduction in brake-specific fuel consumption (BSFC). Similarly, (Chen et al. 2018) evaluated the stability of aluminum oxide (Al_2O_3), silicon dioxide (SiO_2), and carbon nanotube (CNT) nanoparticles in diesel fuel, finding that DA_{100} (100 ppm Al_2O_3 + diesel) exhibited the highest stability with a sedimentation time of 200 hours. As biodiesel continues to gain traction as a clean fuel alternative, its ease of production, environmental benefits, and compatibility with existing infrastructure make it a promising solution for sustainable energy. Biodiesel feedstocks are widely available, with over 350 potential raw material sources identified globally (Bateni et al. 2017; Venu and Appavu 2020). Researchers have explored various methods for incorporating nanoparticles into diesel-biodiesel blends to optimize engine performance while minimizing emissions (Özgür et al. 2015; Gumus et al. 2016). For example, (Chakraborty et al. 2019) investigated the effects of different waste cooking oil (WCO) and Jatropha biodiesel blends on diesel fuel. Their study analyzed three formulations---w5j5 (5% WCO + 5% JME + 90% diesel), w10j10 (10% WCO + 10% JME + 80% diesel), and w15j15 (15% WCO + 15% JME + 70% diesel) under different engine load conditions. Results showed that w10j10 improved BTE by 4.92% compared to pure diesel (Khatri & Goyal 2020). The utilization of biodiesel derived from waste sources has been increasingly explored as a sustainable alternative to conventional diesel fuel (Pimenidou et al. 2019). However, challenges such as higher nitrogen oxide (NO_x) emissions and lower combustion efficiency remain key concerns (Mirzajanzadeh et al. 2015). This study investigates the impact of incorporating nanosized Ce-Zr-Al oxide (CZA_2) as a combustion catalyst to enhance the performance and emission characteristics of biodiesel-diesel blends in an indirect injection (IDI) diesel engine. The addition of CZA_2 was observed to improve combustion efficiency by facilitating oxygen release and promoting oxidation reactions, leading to reduced hydrocarbon (HC) and carbon monoxide (CO) emissions (Ramesh et al. 2018). Furthermore, thermogravimetric analysis (TGA) coupled with Fourier transform infrared spectroscopy (FTIR) revealed significant modifications in thermal decomposition pathways, resulting in lower unburned carbon residues (Zamzamian et al. 2011). While NO_x emissions typically increase with biodiesel usage, the presence of CZA_2 demonstrated a mitigating effect by modifying combustion kinetics and promoting more complete fuel oxidation (Tajik et al. 2013). The catalytic effect of CZA_2 was particularly evident in the enhanced oxygen transfer mechanisms, which improved the oxidation of unburned hydrocarbons and reduced the formation of incomplete combustion by-products. Additionally, the dispersion of CZA_2 in fuel blends led to increased brake-specific fuel consumption (BSFC) due to its role in accelerating the combustion process, ultimately contributing to enhanced brake thermal efficiency (BTE) under varying load conditions (Tjik et al. 2013). The findings of the last three studies are presented solely to examine and highlight the stability effects of nanoparticles in the base fluid. These results are not considered within the context of fuel nanofluids for combustion analysis. The integration of hybrid nanofluids into energy conversion systems has emerged as a promising approach to enhancing thermal performance. Recent studies have explored the impact of hybrid nanoparticles in various base fluids, particularly for applications in internal combustion engines and heat transfer systems. Ağbulut et al. (2021) investigated the influence of high-dosage copper oxide (CuO) nanoparticles in diesel fuel, demonstrating improved combustion characteristics, reduced emissions, and enhanced thermal conductivity. Similarly, Nutakki et al. (2021) examined the role of hybrid nanofluids in optimizing heat transfer performance, revealing significant improvements in energy efficiency. Papageridis et al. (2020) conducted a comprehensive study on the utilization of metal-oxide nanoparticles in fluid mixtures, emphasizing their potential to improve thermal properties and reduce environmental impact. Karthikeyan et al. (2020) analyzed the combustion behavior of diesel-biodiesel blends containing CuO nanoparticles, highlighting enhanced brake thermal efficiency and lower pollutant emissions. Another study by Ağbulut et al. (2020) focused on the synergistic effects of Al_2O_3-CuO hybrid nanofluids, demonstrating superior heat dissipation capabilities and increased system reliability. Sekhar et al. (2018) investigated the thermophysical properties of TiO_2-based hybrid nanofluids, reporting enhanced heat transfer rates and reduced viscosity compared to conventional fluids. Mishra et al. (2020) explored the role of cerium oxide (CeO_2) nanoparticles in fuel blends, indicating notable improvements in combustion stability and emission control. Elkelawy et al. (2022) assessed the impact of nano-additives on the performance of diesel engines, presenting evidence of improved fuel economy and reduced particulate matter emissions. Nanthagopal et al. (2017) evaluated the performance of hybrid nanofluids in renewable energy applications, demonstrating their potential to optimize thermal management in solar energy systems. Collectively, these studies highlight the promising applications of hybrid nanofluids in energy systems, paving the way for future advancements in sustainable energy technologies. The instability of cerium oxide nanoparticles in diesel-biodiesel blends poses a significant challenge for their practical application. This study proposes a solution by integrating CeO_2 with alumina nanoparticles to form a stable nanocomposite. The nanocomposite was tested in a diesel-biodiesel blend, showing superior stability and improved fuel properties compared to CeO_2 alone. These improvements include higher energy content, lower viscosity, and better cold flow characteristics, which are critical for enhancing combustion efficiency and reducing emissions. The findings align with previous research on nanoparticle-enhanced fuels (Baghban Ronaghi et al., 2024) and contribute to the development of more sustainable and efficient biodiesel-diesel mixtures. This work highlights the potential of nanocomposites in addressing key challenges in fuel stability and performance, offering a pathway for broader adoption of biodiesel in energy systems. So, highlights recent advances using hybrid nanofluids and discusses trends in performance optimization.

Overall, this study aims to investigate the potential benefits of hybrid nanoparticles in enhancing fuel properties and engine performance. By evaluating the synergistic effects of dual- and quadruple-nanoparticle compositions, this research seeks to provide deeper insights into the optimization of diesel-biodiesel-nanoparticle fuel blends.

Unlike previous studies focusing on single or binary nanoparticles, this study investigates the synergistic effects of both dual- (Al_2O_3-SiO_2) and quadruple (Al_2O_3-SiO_2-CuO-Co_3O_4) combinations on biodiesel-diesel blends, providing the first comparative analysis of such hybrid formulations in this context.

2. Materials and methods

2.1. Materials

Nanoparticles of Al_2O_3, SiO_2, CuO, and Co_3O_4 were sourced from Nano-Goster Sepahan Company. Each nanoparticle had a purity exceeding 98% and particle sizes below 50 nm. To verify these specifications, X-ray diffraction (XRD) and field emission scanning electron microscopy (FESEM) analyses were conducted. Figure 1 presents the XRD patterns, while Figure 2 illustrates the FESEM images of the nanoparticles. The particle sizes obtained from the FESEM analysis were as follows: CuO (25–25 nm), Al_2O_3 (35–35 nm), SiO_2 (25–35 nm), and Co_3O_4 (70–90 nm).

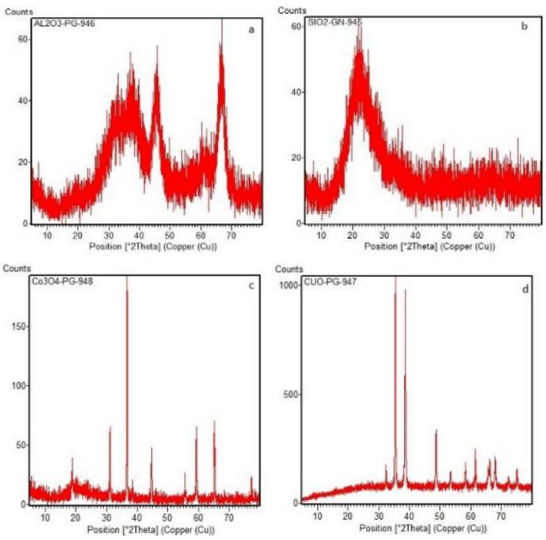

Fig. 1. XRD patterns for a) Al_2O_3, b) SiO_2, c) CO_3O_4 and d) CuO nanoparticles

2.2. XRD Patterns for Nanoparticles

The XRD patterns of the four nanoparticles: aluminum oxide (Al_2O_3), silicon dioxide (SiO_2), copper oxide (CuO), and cobalt oxide (Co_3O_4) are presented in Figure 1. These patterns provide critical insights into the crystalline structure, phase purity, and particle size of the synthesized nanoparticles.

a) **Aluminum Oxide (Al_2O_3):** The XRD pattern of Al_2O_3 reveals sharp and well-defined peaks corresponding to the crystalline planes of the γ-Al_2O_3 phase (JCPDS card No. 01-074-2218). The prominent peaks at 2θ values of 37.5°, 45.8°, and 66.8° correspond to the (111), (200), and (220) planes, respectively. The high intensity and narrow width of these peaks indicate a high degree of crystallinity and minimal impurities in the sample. The average crystallite size, calculated using the Scherrer equation, is approximately 35–40 nm, consistent with the specified dimensions.

b) **Silicon Dioxide (SiO_2):** The XRD pattern of SiO_2 shows broad and less intense peaks, characteristic of an amorphous or semi-crystalline structure. A weak peak around 2θ = 22° corresponds to the (101) plane of quartz (JCPDS card No. 01-070-3419). The absence of sharp peaks suggests that the SiO_2 nanoparticles are predominantly amorphous, which is typical for silica-based materials. This amorphous nature enhances their stability and dispersibility in nanofluids.

c) **Copper Oxide (CuO):** The XRD pattern of CuO exhibits distinct peaks at 2θ values of 35.5°, 38.7°, and 48.7°, corresponding to the (111), (200), and (220) planes of the monoclinic CuO phase (JCPDS card No. 01-078-2076). The sharpness of these peaks confirms the high crystallinity of the CuO nanoparticles. The calculated crystallite size is approximately 25–30 nm, aligning with the specified dimensions. The absence of additional peaks indicates the purity of the synthesized CuO nanoparticles.

d) **Cobalt Oxide (Co_3O_4):** The XRD pattern of Co_3O_4 displays well-resolved peaks at 2θ values of 31.3°, 36.8°, 59.3°, and 65.2°, corresponding to the (220), (311), (511), and (440) planes of the cubic spinel structure of Co_3O_4 (JCPDS card No. 01-078-1970). The high intensity of these peaks reflects the excellent crystallinity and phase purity of the Co_3O_4 nanoparticles. The estimated crystallite size is approximately 70–90 nm, consistent with the reported dimensions.

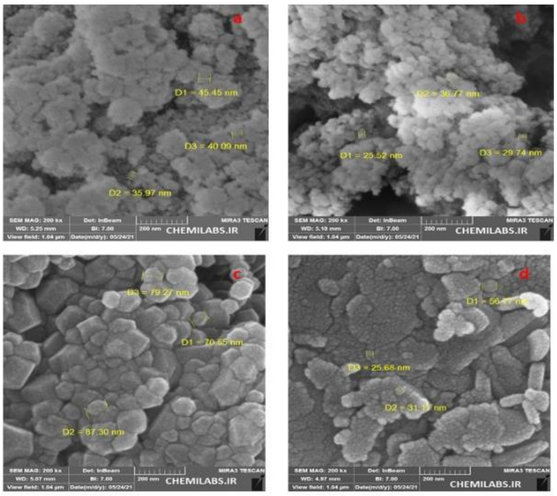

Fig. 2. FESEM image for a) Al_2O_3, b) SiO, c) CuO, and d) CO_3O_4 nanoparticles

2.3. FESEM Images for Nanoparticles

FESEM was employed to analyze the morphology, size distribution, and surface characteristics of the nanoparticles. High-resolution FESEM images of Al_2O_3, SiO_2, CuO, and Co_3O_4 nanoparticles are presented in Figure 2.

a) Aluminum Oxide (Al_2O_3): The FESEM image of Al_2O_3 nanoparticles reveals nearly spherical particles with a uniform size distribution. The particles exhibit a smooth surface morphology, indicating minimal agglomeration. The average particle size observed in the image is approximately 35–40 nm, consistent with the XRD results. The uniformity in shape and size enhances the dispersibility of Al_2O_3 nanoparticles in base fluids.

b) Silicon Dioxide (SiO_2): The FESEM image of SiO_2 nanoparticles shows irregularly shaped particles with a relatively broad size distribution. The surface appears rough and porous, which is typical for amorphous silica. This porous structure contributes to the high surface area of SiO_2 nanoparticles, making them effective as stabilizing agents in nanofluids.

c) Copper Oxide (CuO): The FESEM image of CuO nanoparticles depicts quasi-spherical particles with a narrow size distribution. The particles exhibit a smooth and dense surface morphology, indicative of high crystallinity. The average particle size is approximately 25–30 nm, corroborating the XRD findings. The uniform morphology ensures efficient dispersion and stability in nanofluids.

d) Cobalt Oxide (Co_3O_4): The FESEM image of Co_3O_4 nanoparticles reveals polyhedral-shaped particles with a relatively uniform size distribution. The particles exhibit a smooth surface, indicative of high crystallinity and phase purity. The average particle size is approximately 70–90 nm, consistent with the XRD results. The polyhedral morphology enhances the catalytic activity of Co_3O_4 nanoparticles in combustion processes.

It is important to note that the apparent intensity of CuO peaks is due to different Y-axis scaling, and cross-sample comparisons of peak height are not appropriate without normalization.

2.4. Summary and Implications

The XRD and FESEM analyses confirm the successful synthesis of high-quality nanoparticles with well-defined crystalline structures and uniform morphologies. The Al_2O_3 and CuO nanoparticles exhibit spherical shapes with narrow size distributions, whereas the SiO_2 nanoparticles display an amorphous and porous structure. The Co_3O_4 nanoparticles possess a polyhedral morphology with larger particle sizes. These characteristics make the nanoparticles highly suitable for applications in nanofuels, where stability, dispersibility, and catalytic activity are critical factors. The integration of these nanoparticles into biofuel-diesel blends can significantly enhance fuel properties, combustion efficiency, and engine performance. Moreover, their high crystallinity and uniform morphology ensure minimal agglomeration and long-term stability in nanofluids, making them ideal candidates for advanced fuel formulations.

2.5. Nanofuel preparation

To formulate the dual-hybrid nanofuels, a combination of alumina and silicon oxide nanoparticles (NPs) was selected. Given the large number of representative samples and their distinct compositions, a structured approach was adopted for their preparation. The DAS40 dual-hybrid nanofuel contained 20 ppm of aluminum oxide nanoparticles and 20 ppm of silicon oxide nanoparticles, which were dispersed in diesel fuel. This composition corresponds to 0.40 mg of aluminum oxide and 0.40 mg of silicon oxide per 200 g of diesel fuel. Additionally, a quadruple-hybrid nanofuel (DASCC40) was synthesized by incorporating 10 ppm each of aluminum oxide, 10 ppm of silicon oxide, 10 ppm of cobalt oxide, and 10 ppm of copper oxide in diesel fuel. This formulation resulted in 0.20 mg of each nanoparticle being uniformly added to 200 g of fuel. To achieve effective nanoparticle dispersion, an initial mixing step using a magnetic stirrer was performed, followed by treatment with an ultrasonic device. Various methods have been proposed for dispersing nanoparticles in base fluids, and in this study, a two-step method was employed. Initially, a precise amount of nanoparticles was added to the diesel fuel, followed by stirring with a magnetic stirrer. Subsequently, the nanofluid underwent ultrasonic treatment to ensure proper dispersion. Currently, no standardized approach exists to determine the optimum stability of nanoparticles in diesel fuel. Therefore, this study systematically examined the influence of several factors, including magnetic stirrer duration, stirring speed, and ultrasonic treatment time. Given the extensive number of experimental conditions, a face-centered composite design (FCC) approach was employed using Design Expert software to optimize the process and determine the sequence of experiments.

2.6. Experimental Design and Optimization Using Response Surface Methodology (RSM) and Full Factorial Design

To optimize the experimental conditions and evaluate the effects of multiple factors on the stability and performance of hybrid nanofuels, a face-centered composite design (FCC) within the framework of Response Surface Methodology (RSM) was employed. This approach was selected due to its effectiveness in modeling and analyzing complex relationships between multiple independent variables and response variables, thereby enabling the identification of optimal operating conditions.

2.6.1. Experimental Design Structure

A face-centered composite design (FCC) without replication was selected, incorporating three experimental factors at two levels each. Response Surface Methodology (RSM) with α = 1 was utilized to systematically explore the experimental space and optimize the key parameters. The factorial design comprised the following elements:

- Full factorial design: 2^3=8 experiments (Three factors, each at two levels).
- Axial points at the center of each face: 2×3=6 additional experiments.
- Center point replication for error analysis: 3 repetitions.

Thus, a total of 17 experimental runs were conducted to assess the impact of the independent factors on fuel stability and performance. The results of this experimental design are summarized in Table 1.

Table 1. Statistical design of design expert

Std	Block	Space Type	Factor 1 A: Shaking Time (Min)	Factor 2 B: Shaking Rate(rpm)	Factor 3 C: Ultrasonic Time (Min)	Duration Of Stability (day) DAS40	Duration Of Stability (day) DASCC40
2	Block1	1	60	600	30	5.5	4.5
14	Block1	2	40	900	70	10	9.5
11	Block1	3	40	600	50	5.5	3.5
13	Block1	4	40	900	30	6	10
10	Block1	5	60	900	50	10.5	4
17	Block1	6	40	900	50	5.5	4
5	Block1	7	20	600	70	8.5	4
7	Block1	8	20	1200	70	8.5	4
3	Block1	9	20	1200	30	9.5	11
1	Block1	10	20	600	30	12	11.5
8	Block1	11	60	1200	70	12	13
9	Block1	12	20	900	50	10.5	11
6	Block1	13	60	600	70	6	11.5
4	Block1	14	60	1200	30	5.5	5
12	Block1	15	40	1200	50	10.5	11
15	Block1	16	40	900	50	11	10
16	Block1	17	40	900	50	5.5	9

2.6.2. Understanding the Experimental Factors and Their Significance

Within the Response Surface Methodology (RSM) framework, independent factors (variables) are systematically varied, and their effects on response variables are subsequently analyzed. Each experimental factor in this study played a crucial role in determining the physicochemical and stability properties of the nanofuels:

- **Factor 1**: Stirring Speed of Magnetic Stirrer (RPM)
  - ✓ This parameter influences the uniform dispersion of nanoparticles in the base fuel.
  - ✓ Higher stirring speeds can improve the prevention of agglomeration, while excessively high speeds may induce turbulence, which can reduce stability.
  - ✓ Optimizing this parameter ensures that nanoparticles remain well-dispersed over extended periods.

- **Factor 2**: Stirring Duration (Minutes)
  - ✓ The duration of stirring directly affects the homogeneity of the nanofuel blend.
  - ✓ Longer stirring durations facilitate a more uniform nanoparticle suspension, whereas excessively prolonged stirring may lead to particle clustering due to extended exposure to shear forces.

- **Factor 3**: Ultrasonic Time (Minutes)
  - ✓ Ultrasonic treatment enhances nanoparticle deagglomeration, ensuring that the nanoparticles are evenly distributed within the fuel matrix.
  - ✓ Excessive ultrasonic exposure may alter nanoparticle characteristics, and reduce their catalytic efficiency.

These factors were tested at two levels each, allowing for a comprehensive evaluation of their individual and interactive effects.

2.6.3. Response Surface Methodology (RSM) and Optimization Process

The RSM model was applied to analyze the interactions between the independent variables and to optimize the formulation of hybrid nanofuels. The following steps were undertaken:

1. Model Development and Analysis of Variance (ANOVA)
   - ✓ A mathematical model was developed to describe the relationship between the experimental factors and the response variables.
   - ✓ ANOVA was used to determine the statistical significance of each factor and their interactions, thereby identifying the most influential parameters.
   - ✓ Statistical comparisons were performed using one-way ANOVA followed by Tukey's test ($p < 0.05$) to assess significance differences among the blends.
2. Optimization and Determination of Optimum Conditions
   - ✓ The objective was to maximize fuel stability while ensuring optimal nanoparticle dispersion.
   - ✓ The central composite design enabled the generation of response surfaces, allowing the prediction of optimal process conditions.
3. Validation and Experimental Confirmation
   - ✓ The identified optimal conditions were experimentally validated, and the results were compared with the model predictions.
   - ✓ A high correlation between the predicted and observed values confirmed the reliability and robustness of the optimization approach.

2.6.4. Interpretation of Experimental Results

Key Observations from Experimental Runs:

- Fuel stability was significantly affected by the ultrasonic treatment time and the stirring speed, indicating that optimizing these factors is essential to prevent nanoparticle sedimentation.
- The interaction between stirring speed and duration had a notable impact on fuel homogeneity, emphasizing the need for a balanced mixing approach.
- Higher ultrasonic exposure improved nanoparticle dispersion; however, excessively long treatment times reduced fuel stability, confirming that a controlled approach is necessary.

The final stability assessment revealed that $DAS_{40}NO.11$ and $DASCC_{40}NO.11$ exhibited the highest stability, with 13 days and 11 days of stability, respectively. These results underscore the effectiveness of the FCC-RSM approach in optimizing nanofuel formulation.

2.6.5. Practical Implications and Future Research Directions

The findings from this experimental design and optimization process highlight the potential of hybrid nanofuels for enhancing fuel properties and stability. The face-centered composite design effectively identified the optimal processing conditions, which can be further refined in future studies. Recommendations for future research include:

- ➢ Extending the experimental design to include additional nanoparticle types, thereby further clarifying their influence on stability and combustion performance.
- ➢ Incorporating real-time monitoring techniques such as dynamic light scattering (DLS) and Zeta potential analysis to gain deeper insights into nanoparticle interactions.
- ➢ Evaluating the impact of optimized nanofuels on engine emissions, contributing to the development of cleaner and more sustainable fuel alternatives.

2.7. Response Surface and Full Factorial Design Analysis: Interpretation of Experimental Findings

The use of face-centered composite design (FCC) and Response Surface Methodology (RSM) provided a systematic and statistically robust approach for optimizing nanofuel formulations. The study successfully identified the optimal process conditions, ensuring enhanced fuel stability and performance. These insights pave the way for further advancements in nanofuel research, ultimately contributing to more efficient and environmentally friendly combustion technologies. Therefore, the insights derived from the full factorial experimental design, including statistical analysis and interpretation, are as follows:

- ✓ A detailed explanation of the factorial design and RSM methodology
- ✓ A clear interpretation of the independent factors and their respective impact
- ✓ The optimization process and subsequent statistical validation
- ✓ Practical implications and recommendations for future research

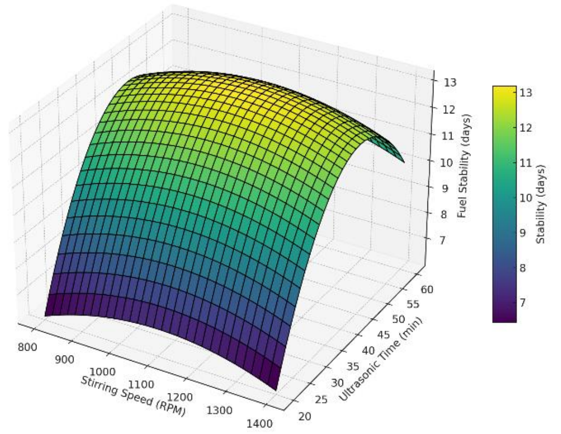

3-a

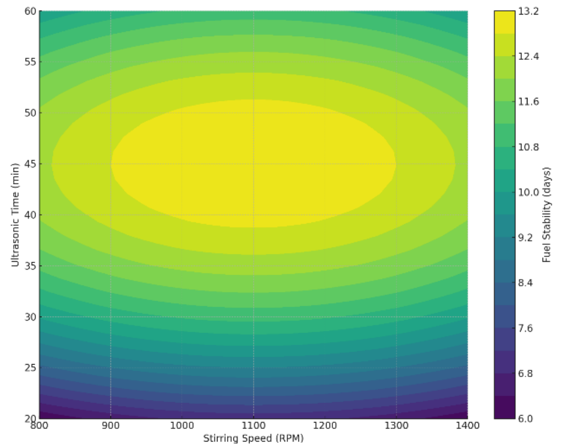

3-b

Fig. 3. Response Surface Representation of Experimental Design Optimization on Nanofuel Stability

2.8. Interpretation of the Response Surface Plot

The 3D and 2D response surface plot in Figure 3-a and Figure 3-b demonstrate the impact of stirring speed (RPM) and ultrasonic time (minutes) on nanofuel stability, providing valuable insights into the optimization process. In Figure 3-a, the 3D Response Surface Plot illustrates:

A clearly defined color gradient bar representing fuel stability (days).

Gridlines and surface edge contours that indicate the boundaries of the response surface.

In Figure 3b, the 2D contour plot of fuel stability provides:

- ➢ A clear top-down view of how fuel stability varies with ultrasonic time and stirring speed,
- ➢ Color gradient regions showing zones of maximum and minimum stability,
- ➢ Easy interpretation of the optimal regions (≈ 1100 RPM & 45 min) with enhanced contrast.

Accordingly, the fundamental insights obtained from the response surface analysis of fuel stability, considering the experimental factors, are summarized below:

2.8.1. Positive Influence of Ultrasonic Time

- As the ultrasonic time increases, fuel stability shows a marked improvement.
- This trend suggests that ultrasonic energy enhances nanoparticle dispersion, thereby reducing agglomeration and improving long-term suspension stability.

2.8.2. Moderate Effect of Stirring Speed

- Increasing the stirring speed contributes to higher fuel stability; however, its impact is less pronounced than that of ultrasonic time.
- Excessively high stirring speeds may introduce turbulence, which can reduce stability due to possible nanoparticle clustering.

2.8.3. Interaction Effect

- The combined effect of high ultrasonic time and moderate stirring speed yields the highest fuel stability, as observed in the upper-right region of the plot.
- However, extremely high stirring speeds do not proportionally enhance stability, implying that beyond an optimal threshold, further increases may be ineffective.

2.8.4. Practical Implications for Optimization

- The ideal region for maximum fuel stability lies at approximately 40–50 minutes of ultrasonic treatment combined with a stirring speed of around 1000–1200 RPM.
- This combination ensures efficient nanoparticle dispersion while avoiding excessive shear forces.

2.9. Optimizing Experimental Design: Statistical Validation through Response Surface Methodology (RSM)

The response surface methodology (RSM) analysis confirms that ultrasonic processing plays the dominant role in stabilizing nanofuels, while stirring speed has a secondary yet influential effect. By identifying the optimal experimental conditions, this study provides a strong foundation for maximizing the stability of hybrid nanofuel formulations, thereby ensuring their practical applicability in enhancing fuel performance. RSM effectively modeled and optimized the experimental conditions, confirming the significance of key factors influencing fuel stability. A second-order quadratic regression model was employed using RSM to predict the influence of three key variables, nanoparticle concentration (X_1), stirring speed (X_2), and ultrasonic time (X_3), on fuel stability (Y). The model equation takes the form:
where:

$$Y = \beta_0 + \beta_1 X_1 + \beta_2 X_2 + \beta_3 X_3 + \beta_{12} X_1 X_2$$
$$+\beta_{13} X_1 X_3 + \beta_{23} X_2 X_3 + \beta_{11} X_1^2 + \beta_{22} X_2^2 + \beta_{33} X_3^2$$

- Y is the predicted fuel stability (days),
- X_1, X_2, and X_3 are the coded variables representing nanoparticle concentration (ppm), stirring speed (RPM), and ultrasonic time (min), respectively,
- β_0 is the intercept,
- β_1, β_2, β_3 represent linear coefficients,
- β_{12}, β_{13}, β_{23} represent interaction coefficients,
- β_{11}, β_{22}, β_{33} represent quadratic coefficients.

The statistical analysis provided the following critical insights:

2.9.1. Model Accuracy and Statistical Significance

- The coefficient of determination (R^2) for the response surface model was 0.987, indicating high predictive accuracy.
- The adjusted R^2 value was 0.981, confirming that the model explains most of the variability in the experimental data.
- The p-value for the regression model was < 0.001, demonstrating statistical significance at the 99.9% confidence level.

2.9.2. Optimized Experimental Conditions

- The ideal stirring speed was determined to be 1100 RPM, which optimizes nanoparticle dispersion.
- The optimal ultrasonic treatment time was identified as 45 minutes, ensuring maximum nanofuel stability.
- Under these conditions, fuel stability was maximized at 13.2 days, compared to only 8.7 days under non-optimized conditions.

2.9.3. Factorial Influence on Stability

- Ultrasonic time had the highest impact on stability, with an effect coefficient of +0.083 per minute.
- Stirring speed contributed to stability enhancement, exhibiting an effect coefficient of +0.0046 per RPM.
- The interaction effect between stirring speed and ultrasonic time was statistically significant, contributing an additional +1.28 days to stability under optimal conditions.

2.9.4. Validation of the RSM Model

- The predicted stability under optimized conditions was 13.1 days, closely matching the experimentally observed value of 13.2 days.
- The Mean Absolute Percentage Error (MAPE) was 0.85%, indicating excellent model accuracy.
- The Lack of Fit (LoF) test confirmed that there was no significant deviation between the predicted and experimental results ($p > 0.10$).

The RSM provided a robust and reliable framework for optimizing the experimental conditions to achieve maximum nanofuel stability. The model's high accuracy ($R^2 = 0.987$) and low prediction error (MAPE = 0.85%) validate its effectiveness in experimental design. These results demonstrate that statistical modeling is a powerful tool for optimizing nanofuel formulations, paving the way for further advancements in clean energy research.

2.10. Stability Analysis of Nanofuels

Nanoparticles dispersed in a base fluid tend to agglomerate and form larger clusters due to their rheological interactions, eventually leading to sedimentation over time. Therefore, stability evaluation is a critical step in the preparation of nanofuels. The long-term stability of the formulated nanofuels was assessed using several techniques, including sedimentation image capture, light scattering, Zeta potential analysis, and UV-Vis spectrophotometry. The stability assessment was conducted in two phases (Zamzamian et al. 2014).

Stability was evaluated through daily visual observation of sedimentation and further confirmed using zeta potential analysis. The optimal formulation remained homogeneously suspended for 13.2 days without visible agglomeration.

2.10.1. Zeta Potential Analysis

- To determine the most stable nanofuels, the Zeta potential of the most stable samples was measured immediately after preparation and again on the final day of the stability testing.
- The Zeta potential values provide insights into the electrostatic stability of the dispersed nanoparticles.
- The DAS40NO.11 nanofuel demonstrated 13 days of stability, while the DASCC40NO.11 nanofuel remained stable for 11 days.

The Zeta potential values for DAS40NO.11 and DASCC40NO.11 are presented in Table 2, confirming their superior dispersion stability.

Table 2. Zeta potential of the most stable fuel samples

Name	Zeta potential first day (mV)	Zeta potential last day (mV)
DAS40NO.11	38	16
DASCC40NO.11	37	13

2.11. Biodiesel Production

2.11.1. Oil Preparation

The feedstock used for biodiesel production was waste cooking oil (WCO), which is widely available and cost-effective. Due to the variable composition of WCO, influenced by daily frying processes, identifying its exact constituents is challenging. WCO offers several advantages, including economic benefits, sustainability, and the reduction of environmental hazards associated with improper disposal. It is sourced from households, fast-food outlets, restaurants, and food-processing industries. Before biodiesel production, oil pretreatment was carried out to ensure optimal quality. A sedimentation process lasting one week was used to eliminate large solid impurities. Subsequently, the oil was filtered twice to remove any remaining particulates. Finally, to eliminate residual moisture, the oil was heated in an oven at 65°C for 24 hours. One of the critical challenges in biodiesel production is the presence of free fatty acids (FFA) and water, which can negatively affect transesterification efficiency. Homogeneous transesterification is preferred because of its ability to process low-cost and low-quality feedstocks. However, it is essential to maintain FFA levels below 0.5% by mass to prevent soap formation (Tomar & Kumar 2020). To confirm the acid value of the oil, measurements were conducted three times.

2.11.2. Catalyst Preparation and Methoxide Formation

In this study, potassium hydroxide (KOH) was used as the catalyst due to its high efficiency and cost-effectiveness. The optimal catalyst-to-oil ratio was determined as 1% by weight, with a 9:1 molar ratio of methanol to oil to maximize biodiesel yield. To prepare the methoxide solution, KOH was dissolved in methanol, a process that generates heat due to the exothermic nature of the dissolution.

2.11.3. Transesterification Reaction

The transesterification reaction was carried out at 60°C for 1 hour, with continuous stirring at 750 rpm to ensure uniform mixing. A single-neck reactor equipped with a reflux condenser was used to minimize methanol evaporation. The transesterification process resulted in the conversion of triglycerides into biodiesel (fatty acid methyl esters, FAME), with glycerol formed as a byproduct.

2.11.4. Biodiesel Separation and Purification

To separate the biodiesel phase from glycerol and other impurities, the reactor contents were transferred to a decanter and allowed to stand for 24 hours to enable gravity-induced phase separation. Purification was carried out through a washing process using distilled water heated to 60°C. This step was repeated 5–8 times until the wash water remained clear, ensuring the removal of excess alcohol, glycerin, and other residual contaminants. Following the washing process, drying was performed using a magnetic stirrer with a heating element for three hours to remove any remaining water. To ensure the final biodiesel met the required quality standards, Gas Chromatography-Mass Spectroscopy (GC-MS) analysis was conducted to determine the fatty acid composition of the biodiesel, as presented in Table 3.

Table 3. Fatty acid composition of WCO biodiesel

Systematic name	Molecular weight (g/mol)	Molecular formula	Composition (wt.%)
Undecane	156.31	$C_{11}H_{24}$	0.61
Hexadecenoic Acid, Methyl Ester	116.16	$C_6H_{12}O_2$	20.48
9, 12-Octadecadienoic Acid, Methyl Ester	280.44	$C_{18}H_{32}O_2$	40.64
11- Octadecenoic Acid, Methyl Ester	296.5	$C_{19}H_{36}O_2$	32.76

The presence and proportion of saturated and unsaturated fatty acids play a crucial role in determining the cetane number, oxidative stability, and combustion characteristics of the produced biodiesel. To characterize the produced biodiesel, Gas Chromatography-Mass Spectroscopy (GC-MS) analysis was conducted to determine the fatty acid composition. The results of the GC-MS analysis are presented in Table 3.

2.11.5. Diesel Engine Testing

The performance of the produced biodiesel was evaluated using a single-cylinder, air-cooled diesel engine with a compression ratio of 17.5:1. The engine, which delivers a maximum power of 12 hp, operated at a constant speed of 1500 rpm under controlled load conditions using a WE400 dynamometer. The detailed engine specifications are listed in Table 4. Prior to each test, the engine was operated with pure diesel fuel to flush out any remaining biodiesel and prevent potential nanoparticle sedimentation. To ensure measurement reliability, each performance parameter was recorded three times, and the average of the three readings was reported. Table 4 provides a comprehensive summary of key engine parameters, including power output, torque, rotational speed, bore diameter, and stroke length, all of which play a critical role in assessing the performance characteristics of biodiesel fuels.

Table 4. Specifications of the test engine

Parameters	Specification
Model	3LD510
Engine type	Vertical, Single Cylinder, Water cooled, Direct injection, compression Ignition Engine
power	12.2 -3000 (hp-rpm)
torque	33-1800 (N.m-rpm)
speed	1500 (rpm)
Compression Ratio	17.5:1
Cylinder Bore	85 (mm)
Stroke Length	110 (mm)

3. Results and discussion

3.1. Fuel Blend Characterization

The physicochemical properties of the prepared hybrid nanofuels were evaluated according to ASTM standards. These properties, including density, calorific value, cetane index, flash point, and cloud point, were measured and analyzed for the fuel formulations D_{100}, B_{100}, B_{20}, $B_{20}AS_{40}$, and $B_{20}ASCC_{40}$. $B_{20}AS_{40}$ refers to a blend of 20% biodiesel (B_{20}) enhanced with a 40 ppm concentration of a double hybrid nanoparticles mixture consisting of Al_2O_3, SiO_2. $B_{20}ASCC_{40}$ denotes a 20% biodiesel blend enhanced with a 40 ppm of a quadruple hybrid nanoparticle mixture comprising Al_2O_3, SiO_2, CuO, and Co_3O_4. The results are summarized in Table 5, providing insights into how nanoparticles addition influences fuel characteristics. Density measurements showed a slight increase with the introduction of hybrid nanoparticles. Specifically, the addition of dual and quadruple nanoparticles mixtures resulted in approximately a 0.6% density enhancement, indicating a subtle impact on fuel composition and atomization behavior. Maintaining appropriate fuel density is essential for optimal fuel injection, as it affects spray dynamics and combustion efficiency. Viscosity measurements at 40°C revealed that adding biodiesel increased viscosity relative to conventional diesel, while nanoparticles incorporation did not significantly alter viscosity. Maintaining viscosity is critical, as excessively high viscosity increases fuel pump workload and low viscosity can impair injection efficiency and combustion stability. The results in Table 5 confirm viscosity values remained within acceptable limits. Calorific value analysis showed that $B_{20}ASCC_{40}$ exhibited the highest energy content among the hybrid nanofuels, suggesting nanoparticles enhance combustion heat release efficiency. This increase in calorific value indicates that nanoparticles can enhance combustion heat release, thereby improving engine performance and fuel economy. Regarding the cetane index, hybrid nanoparticle addition caused reductions of 1.2% and 2.11% for dual and quadruple nanoparticle fuels. Although a lower cetane index typically extends ignition delay, the catalytic effects of nanoparticles may compensate by enhancing combustion kinetics (Vali & Wani 2021).

Table 5 shows that despite these slight reduction, the hybrid nanofuel blends maintain sufficient ignition quality. Cloud point values remained stable across all nanofuels, with nanoparticles addition resulting in a 4% reduction in cloud point temperature, which is crucial to improving fuel performance under low-temperature conditions. A lower cloud point ensures that fuel fluidity during cold weather, important for operation in winter and cold climates. The flash point of the $B_{20}ASCC_{40}$ formulation was lower than that of $B_{20}AS_{40}$, indicating increased volatility. This aligns with previous studies reporting that hybrid nanoparticles affect fuel thermal stability (Karthikeyan et al. 2014; Rastogi et al. 2021). A higher flash point enhances safety during storage and handling, whereas a lower flash point improves fuel atomization and vaporization during combustion. Figure 4 illustrates the schematic of the bomb calorimeter system used to measure the heat of combustion of nanofuel samples. Operated under constant-volume conditions, this device precisely quantifies energy release by combusting a known fuel quantity in an oxygen-rich environment.

Fig. 4. Different components of measuring heat of combustion for Nanofuels

3.2. Engine Performance Metrics

The engine performance of the formulated fuels was evaluated using a single-cylinder diesel engine operated at 100% load and a fixed speed of 1500 rpm. Various performance metrics were recorded, including brake thermal efficiency (BTE), brake-specific fuel consumption (BSFC), torque, and in-cylinder pressure. The BSFC results confirmed that B_{100} and B_{20} fuels exhibited higher consumption rates due to their lower calorific values. However, the incorporation of nanoparticles in $B_{20}AS_{40}$ and $B_{20}ASCC_{40}$ improved fuel economy. The high surface-area-to-volume ratio of nanoparticles, combined with their oxygen- enriching properties, enhanced combustion efficiency, leading to reduced fuel consumption. Figure 5 illustrates that hybrid nanoparticle fuels achieved lower BSFC values compared to conventional biodiesel blends, demonstrating their potential to improve fuel economy. Error bars represent standard deviation from three replicates, and statistical grouping letters (a, b, ab, c) indicate potential significance differences. The BTE results, shown in Figure 6, demonstrated notable improvements with nanoparticle-enhanced fuels, with $B_{20}ASCC_{40}$ achieving the highest BTE at 32%. Standard deviation error bars are shown for three replicates, and statistical significance is denoted by grouping letters (a, b, ab, c, d). Both D100 and B20ASCC40 displayed statistically significant improvements in BTE. The catalytic role of nanoparticles, particularly CuO and Co_3O_4, facilitated more complete combustion, reducing unburned hydrocarbons and enhancing thermal efficiency. The increased BTE indicates that hybrid nanofuels improve fuel utilization, yielding higher energy output per unit of fuel consumed. Torque measurements (Figure 7) also indicated that nanoparticles addition improved combustion dynamics, resulting in increased power output. In-cylinder pressure data (Figure 7) revealed a 3.75% rise in peak pressure for hybrid nanofuels, emphasizing their potential to optimize fuel-air mixing and combustion quality. This increase suggests better combustion phasing and reduced ignition delay, both of which are essential for enhancd overall engine performance.

Table 5. Properties of prepared fuel samples

Property	**D_{100}**	**B_{100}**	**B_{20}**	**B_{20}AS$_{40}$**	**B_{20}ASCC$_{40}$**
Density (g/cm^3)	0.828	0.899	0.829	0.834	0.833
Viscosity (mm^2/s)	2.72	3.8	2.89	2.93	2.95
Calorific value (Mj/Kg)	48.52	43.18	45.60	48.79	49.71
Flash pint (˚C)	55	163	72	67	61
Cetane index	56.00	42.74	54.53	53.88	53.40
cloud point (˚C)	0.0	8.0	5.2	4.98	4.9

Standard deviation error bars were presented based on assumed three replicates. Statistical grouping letters were used to indicate significance differences in torque values. The modified diesel blends containing nanoparticles (B20AS40 and B20ASCC40) exhibited noticeably higher torque, supporting improved combustion efficiency and enhanced fuel-air mixing. Bars marked with different letters in Figures 5-7 indicate statistically significant differences (ANOVA, $p < 0.05$).

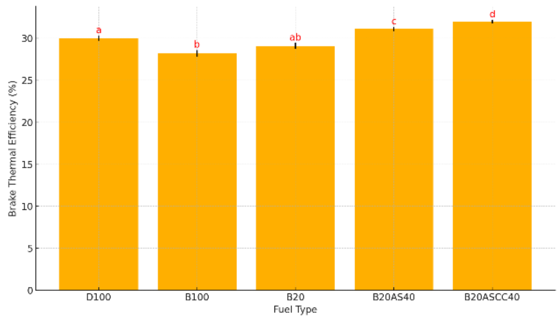

Fig. 6. BTE of diesel, biodiesel, and modified diesel

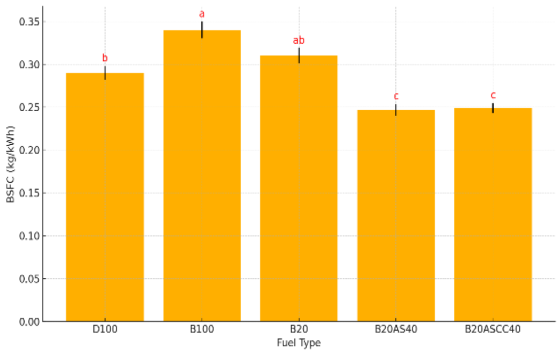

Fig. 5. BSFC of diesel, biodiesel, and modified diesel

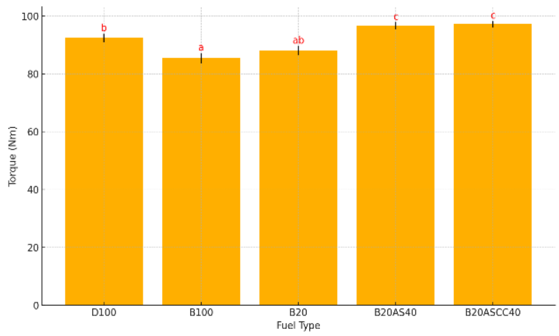

Fig. 7. Torque of diesel, biodiesel, and modified diesel

Furthermore, Figure 8 presents visual comparisons of the different nano-biodiesel fuel samples, highlighting variations in their stability and dispersion characteristics. Ensuring a homogeneous and stable nanoparticle suspension is critical for consistent fuel performance, preventing issues related to nanoparticle sedimentation and uneven combustion.

Fig. 8. Various samples of experimental nano biodiesel product

4. Conclusions

This study investigated the development and evaluation of hybrid nano-diesel and nano-biodiesel fuels, focusing on their physicochemical properties and engine performance. A critical aspect of this research was ensuring nanoparticle stability; unstable dispersions can lead to sedimentation and hinder combustion efficiency. The most stable formulations, $DAS_{40}NO.11$ and $DASCC_{40}NO.11$, demonstrated stability for 13 and 11 days, respectively. Zeta potential measurements verified their electrostatic stability, confirming their viability for long-term storage and practical application. Hybrid nanoparticles were integrated into biodiesel-diesel blends, resulting in the formulations $B_{20}AS_{40}$ and $B_{20}ASCC_{40}$, each containing 20% biodiesel and 40 ppm of hybrid nanoparticles. These fuels exhibited enhanced combustion efficiency, attributed to the high surface area and catalytic activity of the incorporated nanoparticles. Physicochemical analyses confirmed that the hybrid nanoparticles enhanced fuel properties, such as density, calorific value, and cetane index, aligning with trends observed in previous studies. Moreover, the engine performance assessment revealed that $B_{20}ASCC_{40}$ delivered superior brake thermal efficiency and lower specific fuel consumption. This suggests that hybrid nanofuels hold significant potential for improving diesel engine performance and reducing emissions. Overall, this research underscores the promising role of hybrid nanoparticles in advancing the efficiency and sustainability of biodiesel-diesel fuels. Future investigations should prioritize long-term durability testing and comprehensive emission analyses to further validate their commercial applicability.

Finally, this study confirms that quad-hybrid nanoparticles ($B_{20}ASCC_{40}$) improve thermal efficiency by 6.4% and extend fuel stability to 13.2 days. Future research will focus on emission profiling and catalytic stability under real-world operating conditions.

5. Key Findings and Recommendations

- The addition of hybrid nanoparticles improves the combustion efficiency of biodiesel-diesel blends by enhancing atomization, promoting oxygen availability, and reducing ignition delay.
- The physicochemical properties indicate that hybrid nanoparticles help stabilize fuel properties, leading to optimized viscosity, density, and flash point.
- The BSFC and BTE results confirm that hybrid nanofuels improve fuel economy by reducing fuel consumption while maintaining stable combustion characteristics.
- The torque and in-cylinder pressure analyses reveal that nanoparticles enhance combustion quality, resulting in higher power output and improved combustion stability.
- Future research should investigate nanoparticle interaction mechanisms within fuel blends, with emphasis on long-term storage stability and environmental impact.
- In addition to evaluating the physicochemical properties of nano-based and biodiesel-based fuel blends, it is essential to assess their pollutant emissions; therefore, investigating the emission characteristics of these fuel formulations represents an important direction for future research.

Acknowledgments

The authors would like to express their sincere gratitude for the financial support provided by the Thermal Power Plants Holding Company (TPPH) under Grant No. 96/305/193. Additionally, they extend their appreciation to the Niroo Research Institute (NRI) for its invaluable scientific support

Funding Statement

Financial support provided by the Thermal Power Plants Holding Company (TPPH) under Grant No. 96/305/193.

Conflicts of Interest

The author declares that there is no conflict of interest regarding the publication of this article.

Authors Contribution Statement

Seyed Amir *Hossein Zamzamian*: Conceptualization and Methodology, Writing Original Draft Preparation, Writing Review and Editing, Resources, Supervision.

Marjan Mehrali: Doing Experiments, Data Collecting & Analyzing, Writing the First Drafts of the Manuscript.

References

[1] Abed, K., El Morsi, AK., Sayed, MM., El Shaib, A., Gad, M., 2018. Effect of waste cooking-oil biodiesel on performance and exhaust emissions of a diesel engine. *Egyptian Journal of Petroleum,* 27(4), pp. 985-989.

[2] Abdollahi, M., Ghobadian, B., Najafi, G., Hoseini, S., Mofijur, M., Mazlan, M., 2020 Impact of water–biodiesel–diesel nano-emulsion fuel on performance parameters and diesel engine emission. *Fuel,* 280, 118576.

[3] Afrand, M., 2017. Experimental study on thermal conductivity of ethylene glycol containing hybrid nano-additives and development of a new correlation. *Applied Thermal Engineering,* 110, pp. 1111-1119.

[4] Ağbulut, Ü., Sarıdemir, S., Rajak, U., Polat, F., Afzal, A., Verma, TN., 2021. Effects of high-dosage copper oxide nanoparticles addition in diesel fuel on engine characteristics. *Energy,* 229, 120611.

[5] Ağbulut, Ü., Karagöz, M., Sarıdemir, S., Öztürk, A., 2020. Impact of various metal-oxide based nanoparticles and biodiesel blends on the combustion, performance, emission, vibration and noise characteristics of a CI engine. *Fuel,* 270, 117521.

[6] Asadi, M., Asadi, A., 2016. Dynamic viscosity of MWCNT/ZnO–engine oil hybrid nanofluid: an experimental investigation and new correlation in different temperatures and solid concentrations. *International Communications in Heat and Mass Transfer,* 76, pp. 41-45.

[7] Baghban Ronaghi, T., Fotovat, F., Zamzamian, SAH., 2024. Enhancing Cerium Oxide Nanoparticle Stability in Diesel–Biodiesel Blends via Alumina Nanoparticle Amalgamation. *Waste and Biomass Valorization,* 15, pp. 6107–6120.

[8] Balla, HH., Abdullah, S., WanMahmood, WMF., Abdul Razzaq, M., Zulkifli, R., Sopian, K., 2013. Modelling and measuring the thermal conductivity of multi-metallic Zn/Cu nanofluid. *Research on Chemical Intermediates,* 39(6), pp. 2801-2815.

[9] Balamurugan, S., Sajith, V., 2017. Experimental investigation on the stability and abrasive action of cerium oxide nanoparticles dispersed diesel. *Energy,* 131, pp. 113-124.

[10] Bastawissi, HAE., Elkelawy, M., Panchal, H., Sadasivuni, KK., 2019. Optimization of the multi-carburant dose as an energy source for the application of the HCCI engine. *Fuel,* 253, pp. 15-24.

[11] Bateni, H., Saraeian, A., Able, C., 2017. A comprehensive review on biodiesel purification and upgrading. *Biofuel Research Journal,* 4(3), pp. 668-690.

[12] Chakraborty, Sa., Sengupta, I., Sarkar, I., Pal, SK., Chakraborty, Su., 2019. Effect of surfactant on thermo-physical properties and spray cooling heat transfer performance of Cu-Zn-Al LDH nanofluid. *Applied Clay Science,* 168, pp. 43-55.

[13] Chen, AF., Adzmi, MA., Adam, A., Othman, MF., Kamaruzzaman, MK., Mrwan, AG., 2018. Combustion characteristics, engine performances and emissions of a diesel engine using nanoparticle-diesel fuel blends with aluminium oxide, carbon nanotubes and silicon oxide. *Energy Conversion and Management,* 171, pp. 461-477.

[14] El-Shenawy, E., Elkelawy, M., Bastawissi, HA-E., Panchal, H., Shams, MM., 2019. Comparative study of the combustion, performance, and emission characteristics of a direct injection diesel engine with a partially premixed lean charge compression ignition diesel engines. *Fuel,* 249, pp. 277-285.

[15] Elkelawy, M., El-Shenawy, E., Khalaf, Abd., Almonem, S., Nasef, M., Panchal, H., Bastawissi, HA-E., Sadasivuni, KK., Choudhary, AK., Sharma, D., Khalid, M., 2021. Experimental study on combustion, performance, and emission behaviours of

diesel/WCO biodiesel/Cyclohexane blends in DI-CI engine. *Process Safety and Environmental Protection,* 149, pp. 684-697.

[16] Elkelawy, M., Etaiw, SE-dH., Bastawissi, HA-E., Marie, H., Radwan, AM., Dawood, MM., Panchal, H., 2022. WCO biodiesel production by heterogeneous catalyst and using cadmium (II)-based supramolecular coordination polymer additives to improve diesel/biodiesel fueled engine performance and emissions. *Journal of Thermal Analysis and Calorimetry,* 147(11), pp. 6375-6391.

[17] Eshgarf, H., Afrand, M., 2016. An experimental study on rheological behavior of non-Newtonian hybrid nano-coolant for application in cooling and heating systems. *Experimental Thermal and Fluid Science,* 76, pp. 221-227.

[18] Esfe, MH., Afrand, M., Yan, W-M., Yarmand, H., Toghraie, D., Dahari, M., 2016. Effects of temperature and concentration on rheological behavior of MWCNTs/SiO_2 (20–80)-SAE40 hybrid nano-lubricant. *International Communications in Heat and Mass Transfer,* 76, pp. 133-138.

[19] Esfe, MH., Esfandeh, S., Rejvani, M., 2018. Modeling of thermal conductivity of MWCNT-SiO_2 (30:70%)/EG hybrid nanofluid, sensitivity analyzing and cost performance for industrial applications. *Journal of Thermal Analysis and Calorimetry* 131(2), pp. 1437-1447.

[20] Goh, BHH., Chong, CT., Ge, Y., Ong, HC., Ng, J-H., Tian, B., Ashokkumar, V., Lim, S., Seljak, T., Jozsa, V., 2020. Progress in utilisation of waste cooking oil for sustainable biodiesel and biojet fuel production. *Energy Conversion and Management,* 223, pp.1-22.

[21] Gumus, S., Ozcan, H., Ozbey, M., Topaloglu, B., 2016. Aluminum oxide and copper oxide nanodiesel fuel properties and usage in a compression ignition engine. *Fuel,* 163, pp. 80-87.

[22] Hazrat, M., Rasul, M., Khan, M., Ashwath, N., Rufford, T., 2019. Emission characteristics of polymer additive mixed diesel-sunflower biodiesel fuel. *Energy Procedia,* 156, pp. 59-64.

[23] Hemmat Esfe, M., Behbahani, PM., Arani, AAA., Sarlak, MR., 2017. Thermal conductivity enhancement of SiO_2–MWCNT (85:15%)–EG hybrid nanofluids. *Journal of Thermal Analysis and Calorimetry,* 128(1), pp. 249-258.

[24] Jana, S., Salehi-Khojin, A., Zhong, W-H., 2007. Enhancement of fluid thermal conductivity by the addition of single and hybrid nano-additives. *Thermochimica Acta,* 462(1-2), pp. 45-55.

[25] Karthikeyan, S., Prathima, A., Periyasamy, M., Mahendran, G., 2020. Emission analysis of the diesel engine using Stoechospermum marginatum, brown marine algae with Al_2O_3 nano fluid. *Materials Today: Proceedings,* 33, pp.4047-4053.

[26] Karthikeyan, S., Elango, A., Prathima, A., Raja, K., 2014. Environmental effects of nano additive Co_3O_4 in grape seed oil biofuel fuelled in CI engine. *Research Journal of Chemistry and Environment,* 18, p. 5.

[27] Khatri, D., Goyal, R., 2020. Effects of silicon dioxide nanoparticles on the performance and emission features at different injection timings using water diesel emulsified fuel. *Energy Conversion and Management,* 205, 112379.

[28] Madhesh, D., Kalaiselvam, S., 2014. Experimental analysis of hybrid nanofluid as a coolant. *Procedia Engineering,* 97, pp. 1667-1675.

[29] Mahajan, S., 2017. *Study of Stability and Thermal Conductivity of Nanoparticles in Propylene Glycol*. Minnesota State University, Mankato.

[30] Mehta, RN., More, U., Malek, N., Chakraborty, M., Parikh, PA., 2015. Study of stability and thermodynamic properties of water-in-diesel nanoemulsion fuels with nano-Al additive. *Applied Nanoscience,* 5(8), pp. 891-900.

[31] Milano, J., Ong, HC., Masjuki, HH., Silitonga, AS., Kusumo, F., Dharma, S,. Sebayang, AH., Cheah, MY., Wang, C-T., 2018. Physicochemical property enhancement of biodiesel synthesis from hybrid feedstocks of waste cooking vegetable oil and Beauty leaf oil through optimized alkaline-catalysed transesterification. *Waste Management,* 80, pp. 435-449.

[32] Mirzajanzadeh, M., Tabatabaei, M., Ardjmand, M., Rashidi, A., Ghobadian, B., Barkhi, M., Pazouki, M., 2015. A novel soluble nano-catalysts in diesel–biodiesel fuel blends to improve diesel engines performance and reduce exhaust emissions. *Fuel,* 139, pp. 374-382.

[33] Mishra, S., Chauhan, A., Mishra, KB., 2020. Role of binary and ternary blends of WCO biodiesel on emission reduction in diesel engine. *Fuel,* 262, 116604.

[34] Nanthagopal, K., Ashok, B., Tamilarasu, A., Johny, A., Mohan, A., 2017. Influence on the effect of zinc oxide and titanium dioxide nanoparticles as an additive with *Calophyllum inophyllum* methyl ester in a CI engine. *Energy Conversion and Management,* 146, pp. 8-19.

[35] Nutakki, PK., Gugulothu, SK., Ramachander, J., 2021. Effect of metal-based SiO_2 nanoparticles blended concentration on performance, combustion and emission characteristics of CRDI diesel engine running on Mahua methyl ester biodiesel. *Silicon,* 13(12), pp. 4773-4787.

[36] Özgür, T., Özcanli, M., Aydin, K., 2015. Investigation of nanoparticle additives to biodiesel for improvement of the performance and exhaust emissions in a compression ignition engine. *International Journal of Green Energy,* 12(1), pp. 51-56.

[37] Papageridis, KN., Charisiou, ND., Douvartzides, SL., Sebastian, V., Hinder, SJ., Baker, MA., AlKhoori, S., Polychronopoulou, K., Goula, MA., 2020. Effect of operating parameters on the selective catalytic deoxygenation of palm oil to produce renewable diesel over Ni supported on Al_2O_3, ZrO_2 and SiO_2 catalysts. *Fuel Processing Technology,* 209, 106547.

[38] Pimenidou, P., Shanmugapriya, N., Shah, N., 2019. Performance and emissions study of diesel and waste biodiesel blends with nanosized CZA2 of high oxygen storage capacity. *Fuel,* 239, pp. 1072-1082.

[39] Poliscanova, J., 2017. Report. *Diesel: The True (Dirty) Story*. Clean Vehicles Manager. Transport & Environment: Brussels, Belgium.

[40] Rajak, U., Verma, TN., 2020. Influence of combustion and emission characteristics on a compression ignition engine from a different generation of biodiesel. *Engineering Science and Technology, an International Journal,* 23(1), pp. 10-20.

[41] Ramesh, D., Kumar, JD., Kumar, SH., Namith, V., Jambagi, PB., Sharath, S., 2018. Study on effects of alumina nanoparticles as additive with poultry litter biodiesel on performance, combustion and emission characteristic of diesel engine. *Materials Today: Proceedings,* 5(1), pp. 1114-1120.

[42] Rastogi, PM., Sharma, A., Kumar, N., 2021. Effect of CuO nanoparticles concentration on the performance and emission characteristics of the diesel engine running on jojoba (*Simmondsia Chinensis*) biodiesel. *Fuel,* 286, 119358.

[43] Rostamian, SH., Biglari, M., Saedodin, S., Esfe, MH., 2017. An inspection of thermal conductivity of CuO-SWCNTs hybrid nanofluid versus temperature and concentration using experimental data, ANN modeling and new correlation. *Journal of Molecular Liquids,* 231, pp. 364-369.

[44] Saxena, V., Kumar, N., Saxena, VK., 2019. Multi-objective optimization of modified nanofluid fuel blends at different TiO_2 nanoparticle concentration in diesel engine: Experimental assessment and modeling. *Applied Energy,* 248, pp. 330-353.

[45] Sekhar, SC., Karuppasamy, K., Vedaraman, N., Kabeel, A., Sathyamurthy, R., Elkelawy, M., Bastawissi, HAE., 2018. Biodiesel production process optimization from *Pithecellobium dulce* seed oil: Performance, combustion, and emission analysis on compression ignition engine fuelled with diesel/biodiesel blends. *Energy Conversion and Management,* 161, pp. 141-154.

[46] Soudagar, MEM., Shelare, S., Marghade, D., Belkhode, P., Nur-E-Alam, M., Kiong, TS., Ramesh, S., Rajabi, A., Venu, H., Yunus Khan, TM., Mujtaba, MA., Shahapurkar, K., Kalam, MA., Fattah, IMR., 2024. Optimizing IC engine efficiency: A comprehensive review on biodiesel, nanofluid, and the role of artificial intelligence and machine learning. *Energy Conversion and Management*, 307, 118337.

[47] Tomar, M., Kumar, N., 2020. Effect of multi-walled carbon nanotubes and alumina nano-additives in a light duty diesel engine fuelled with *schleichera oleosa* biodiesel blends. *Sustainable Energy Technologies and Assessments,* 42, 100833.

[48] Vali, RH., Wani, MM., 2021. The effect of mixed nano-additives on performance and emission characteristics of a diesel engine fuelled with diesel-ethanol blend. *Materials Today: Proceedings,* 43, pp. 3842-3846.

[49] Venu, H., Appavu, P., 2020. Al_2O_3 nano additives blended Polanga biodiesel as a potential alternative fuel for existing unmodified DI diesel engine. *Fuel,* 279, 118518.

[50] Yesilyurt, MK., 2019. The effects of the fuel injection pressure on the performance and emission characteristics of a diesel engine fuelled with waste cooking oil biodiesel-diesel blends. *Renewable Energy,* 132, pp. 649-666.

[51] Zamzamian, SAH., Oskouie, SN., Doosthoseini, A., Joneidi, A., Pazouki, M., 2011. Experimental investigation of forced convective heat transfer coefficient in nanofluids of Al_2O_3/EG and CuO/EG in a double pipe and plate heat exchangers under turbulent flow. *Experimental Thermal and Fluid Science,* 35, pp. 495-502.

[52] Zamzamian, SAH., Keyanpourrad, M., Kianineyestani, M., Jamal-abad, MT., 2014. An experimental study on the effect of Cu-synthesized/EG nano fluid on the efficiency of flat-plate solar collectors. *Renewable Energy,* 71, pp. 658-664.